Supplementary data

10-MV X-ray dose calculation in water for MLC and wedge fields using a convolution method with X-ray spectra reconstructed as a function of off-axis distance

Akira Iwasaki, Shigenobu Kimura, Kohji Sutoh, Kazuo Kamimura, Makoto Sasamori, Morio Seino, Fumio Komai, Masafumi Takagi, Shingo Terashima, Yoichiro Hosokawa, Hidetoshi Saitoh and Masanori Miyazawa

http://dx.doi.org/10.14312/2399-8172.2017-4

Appendix A

Primary and scatter dose kernels ($H_{1,2}$ and $K_{1,2}$)

On referring to Figure A1, Iwasaki [5] and Iwasaki and colleagues [6] defined $H_{1,2}$ and $K_{1,2}$ functions used for teletherapy radiation beams as follows:

$H_1(\Xi, R; E_N)$ and $H_2(H, R; E_N)$ express the forward and backward primary dose components to points (Ξ, R) and (H, R), respectively, in semi-infinite water phantoms. They are produced at the corresponding origins (O's), per unit water collision kerma caused by the incident E_N photons and per unit volume, setting the incident photon ray line to coincide with the Ξ or H axis. In the same way, we let $K_1(\Xi, R; E_N)$ and $K_2(H, R; E_N)$ be related to the in-water forward and backward scatter dose components, respectively. According to the irradiation geometries, we can have $H_1(0, R; E_N)=H_2(0, R; E_N)$ and $K_1(0, R; E_N)=K_2(0, R; E_N)$.

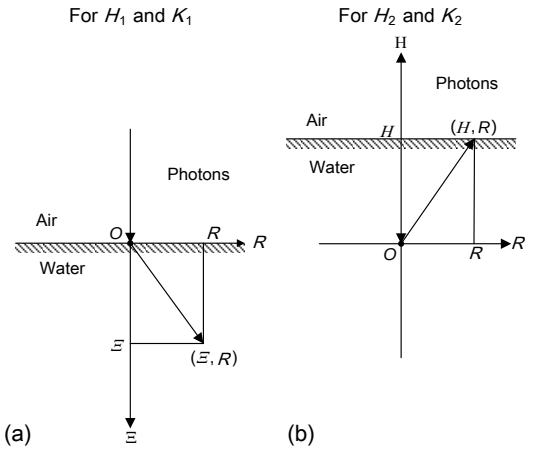

Figure A1 Diagrams showing how (a) the forward component (H_1 or K_1) of the primary and scatter dose kernels for point (Ξ, R) and (b) the backward component (H_2 or K_2) of the primary and scatter dose kernels for point (H, R) should be obtained in semi-infinite water phantoms for incident photons, where the interaction point is situated at point O.

Appendix B

Δϕ, Δθ and Δr′ steps for the polar coordinate system (r′, ϕ, θ)

In order numerically to integrate Equations 1−3 for evaluation of the primary, scatter and contamination doses at point $P(X_C, Y_C, Z_C)$ (Figure 2), we use two other coordinate systems besides the beam coordinate system (X_{beam}, Y_{beam}, Z_{beam}). One is the orthogonal coordinate system (xv, yv, zv) with the origin at point P (it should be noted that the (x_v, y_v, z_v) coordinate system just coincides with the (X_{beam}, Y_{beam}, Z_{beam}) coordinate system when point P coincides with the isocenter (O)), and the other is the polar coordinate system (r', ϕ, θ) derived from the (x_v, y_v, z_v) coordinate system.

Here we use a phantom whose surface is convex in shape for simplicity. Using r', $\Delta\phi$ and $\Delta\theta$, we make a quadrangular pyramid whose apex is located at point P. Then we set small volumes (ΔV's) (using $\Delta r'$'s) in sequence inside the pyramid and a small area (ΔS) at the site of the phantom surface. With respect to the r', ϕ and θ steps, we use the following procedures:

(a) For ϕ steps ($0 \le \phi \le 2\pi$), we set $\Delta\phi_j$=const (j=1, 2, 3, ...).

(b) For θ steps ($0 \le \theta \le \pi$), we set

$$\Delta\theta_k = \Delta\theta_{\min} + \frac{(\Delta\theta_{\max} - \Delta\theta_{\min})}{2}\left[1 - \cos\left\{\pi\left(1 - \exp\left(-\frac{\ln 2}{\theta_H}\theta_{k-1}\right)\right)\right\}\right], \quad \text{(B1)}$$

with k=1, 2, 3, ..., where θ_H is a constant. Let θ_0=0 and $\theta_k = \theta_{k-1} + \Delta\theta_k$; then we have $\Delta\theta_1 = \Delta\theta_{\min}$ and $\Delta\theta_\infty = \Delta\theta_{\max}$ (the step increases slowly at small and large k numbers).

(c) r' steps ($0 \le r'$) are taken within the phantom as

$$\Delta r'_i = \Delta r'_{\min} + \frac{(\Delta r'_{\max} - \Delta r'_{\min})}{2}\left[1 - \cos\left\{\pi\left(1 - \exp\left(-\frac{\ln 2}{r'_H} r'_{i-1}\right)\right)\right\}\right], \quad \text{(B2)}$$

with i=1, 2, 3, ..., where $\Delta r'_H$ is a constant. Let $\Delta r'_0$=0 and $r'_i = r'_{i-1} + \Delta r'_i$; then we have

$\Delta r_1'=\Delta r_{\min}'$ and $\Delta r_\infty'=\Delta r_{\max}'$ (the step increases slowly at small and large *i* numbers). Each *r'* axis is drawn through the centers of $\Delta\theta_j$ and $\Delta\theta_k$. Within each delta volume (ΔV), we set an effective point on the *r'*-axis. For example, the effective point for the *i*th ΔV is placed at a distance of $(r_i' - f_V \Delta r_i')$ from point *P*, where f_V is the shifting factor ($0 \leq f_V \leq 1$), letting it be a constant for any set of (*i*, *j*, *k*), depending on the primary or scatter dose calculations. The effective point is taken for evaluation of representative values within each ΔV with respect to the primary or scatter dose kernel (h_{phan} or k_{phan}) and the primary water collision kerma ($K_{\text{water}}^{\text{MLC}}$) in Equations 1 and 2. For the ratio of $\mu_{\text{phan}}/\mu_{\text{water}}$ in Equations 1 and 2, we take the ratio value averaged within each ΔV.

For the present 10-MV X-ray dose calculations the following data sets were adopted: For the primary and electron contamination dose calculations, we used a data set of f_V=0.415, $\Delta r_{\min}'$=0.01 cm, $\Delta r_{\max}'$=0.65 cm, r_{H}'=0.406 cm, $\Delta\phi_j$ =0.0436 rad (=2.5°), $\Delta\theta_{\min}$=0.0175 rad (=1.0°), $\Delta\theta_{\max}$=0.0524 rad (=3.0°) and θ_{H}=0.2983 rad (=17.09°). For the scatter dose calculations, we used a data set of f_V =0.01, $\Delta r_{\min}'$=0.25 cm, $\Delta r_{\max}'$=2.0 cm, r_{H}'=11.439 cm, $\Delta\phi_j$=0.0436 rad (=5.0°), $\Delta\theta_{\min}$=0.0175 rad (=1.0□), $\Delta\theta_{\max}$=0.0698 rad (=4.0°) and θ_{H}=1.0949 rad (=62.73°). It should be noted that the f_V values were determined by comparison of calculated and measured percentage depth dose (PDD) data in water, where the values of f_V=0.415 and f_V=0.01 were determined mainly for small and large fields, respectively.

Appendix C

Definitions of the off-center jaw-S_c factor, the MLC-S_c factor, the jaw-S_c factor and the off-center MLC-S_c factor

Here we describe other deals using Equation 23, where the calculation point (X_0, Y_0), the jaw field (A_{jaw}) and the MLC field (A_{MLC}) are assessed on the isocenter plane. When the MLC is removed

from an open A_{MLC} field under a given A_{jaw} field, we should put $A_{\mathrm{MLC}} = \infty$ and $A_{\mathrm{MLC}}^{\mathrm{black}} = 0$. Then the term in the brackets of the right side of Equation 23 can be rewritten as

$$S_{\mathrm{c\_center}}(X_0, Y_0; A_{\mathrm{MLC}} = \infty, A_{\mathrm{jaw}}) = H_{\mathrm{jaw}}(X_0, Y_0; A_{\mathrm{jaw}}) / H_{\mathrm{jaw}}(0,0; 10 \times 10_{\mathrm{iso}}). \quad \text{(C1)}$$

This factor may be called the "off-center jaw-S_c factor."

Alternatively, if the in-air beam intensity is normalized at a fixed point (X_0, Y_0) by using an open jaw field of $A_{\mathrm{jaw}} = 10 \times 10\ \mathrm{cm}^2$ whose center is at the fixed point (X_0, Y_0), then the collimator scatter factor (S_c) at the fixed point (X_0, Y_0) for an open A_{MLC} field under a given A_{jaw} field can be formulated as

$$S_{\mathrm{c}}(X_0, Y_0; A_{\mathrm{MLC}}, A_{\mathrm{jaw}}) = \left[H_{\mathrm{jaw}}(X_0, Y_0; A_{\mathrm{jaw}}) - H_{\mathrm{MLC}}^{\mathrm{black}}(X_0, Y_0; A_{\mathrm{MLC}}^{\mathrm{black}})\right] / H_{\mathrm{jaw}}(X_0, Y_0; 10 \times 10).) \quad \text{(C2)}$$

This factor may be called the "MLC-S_c factor."

When the MLC is removed from the beam, Equation C2 can be rewritten as

$$S_{\mathrm{c}}(X_0, Y_0; A_{\mathrm{MLC}} = \infty, A_{\mathrm{jaw}}) = H_{\mathrm{jaw}}(X_0, Y_0; A_{\mathrm{jaw}}) / H_{\mathrm{jaw}}(X_0, Y_0; 10 \times 10). \quad \text{(C3)}$$

This factor may be called the "jaw-S_c factor."

In particular, when normalization is performed at the isocenter, another type of S_c factor can be formulated as

$$S_{\mathrm{c\_iso}}(X_0, Y_0; A_{\mathrm{MLC}}, A_{\mathrm{jaw}}) = \left[H_{\mathrm{jaw}}(X_0, Y_0; A_{\mathrm{jaw}}) - H_{\mathrm{MLC}}^{\mathrm{black}}(X_0, Y_0; A_{\mathrm{MLC}}^{\mathrm{black}})\right] / H_{\mathrm{jaw}}(0,0; 10 \times 10_{\mathrm{iso}}). \quad \text{(C4)}$$

This factor may be called the "off-center MLC-S_c factor."

Appendix D

The beam intensity correction factor of $\mathrm{CF}_{\mathrm{OPF}}^{\mathrm{a}}$

This Appendix is described using 10-MV X-ray beams from the present linear accelerator equipped with MLC and wedge devices supplied by the manufacturer. The beam irradiations are performed using "open or wedge-filtered jaw fields with or without MLC."

The $\mathrm{CF}_{\mathrm{OPF}}^{\mathrm{a}}$ factor in Equations 43 and 46 works on ΔS and ΔV elements (related to the phantom) as a beam intensity correction used for the in-air OPF calculation of $\mathrm{OPF}_{\mathrm{in\_air}}^{\mathrm{single}}$ or $\mathrm{OPF}_{\mathrm{in\_air}}^{\mathrm{multi}}$. The present study does not use such corrections for ΔV_L elements $(L = 1, 2, \cdots, L_{\max})$ within the MLC and wedge devices (Figure 8) because the primary and scatter dose components from these devices are relatively small when compared with those from ΔS and ΔV elements

related to the phantom. The $\mathrm{CF}^{\mathrm{a}}_{\mathrm{OPF}}$ factor gives the same correction to any point (X_0, Y_0) set on the isocenter plane (Figure 8) under a given value of $A^{\mathrm{in\_jaw}}_{\mathrm{MLC}}/A_{\mathrm{jaw}}$ and under a given number of the irradiation modes (wedge type $= 0 - 4$).

Next we construct four series of $\mathrm{CF}^{\mathrm{a}}_K$, $\mathrm{dev}^{\%}_K$, $f^{\%}_K$ and W_K $(K = 0, 1, 2, \cdots)$ based on calculated and measured PDD datasets at a depth of *Z*=3 cm of water with a reference depth of Z_{R}=10 cm (Equation 52), letting $\mathrm{CF}^{\mathrm{a}}_K$ denote a *K*-series regarding the $\mathrm{CF}^{\mathrm{a}}_{\mathrm{OPF}}$ factor, $\mathrm{dev}^{\%}_K$ denote a *K*-series reflecting % deviations of the calculated PDD datasets, $f^{\%}_K$ denote a *K*-series reconstructed as $f^{\%}_K = 1 - \mathrm{dev}^{\%}_K/100$, and W_K denote a *K*-series regarding a specific item that appears while handling the $\mathrm{CF}^{\mathrm{a}}_K$ expressions (Equations D2, D6, D9 and D12). Each of the *K*-series is treated as a function of $A^{\mathrm{in\_jaw}}_{\mathrm{MLC}}/A_{\mathrm{jaw}}$ and wedge type. To avoid mathematical impossibility in the following expressions of Equations D5 and D9 containing $A^{\mathrm{in\_jaw}}_{\mathrm{MLC}}/A_{\mathrm{jaw}}$ in the denominators, we set $A^{\mathrm{in\_jaw}}_{\mathrm{MLC}}/A_{\mathrm{jaw}} = 0.999$ for $A^{\mathrm{in\_jaw}}_{\mathrm{MLC}}/A_{\mathrm{jaw}} \geq 0.999$. However, relatively wide distributions of the $\mathrm{dev}^{\%}_K$ data at $A^{\mathrm{in\_jaw}}_{\mathrm{MLC}}/A_{\mathrm{jaw}} = 0.999$, as shown in Figure D1 (described below), demonstrates that the MLC leaves, even outside the jaw field, seem to have some effects on the dose measurement.

The PDD datasets were produced as follows: (a) in case of wedge type = 0 (no wedge), we used no MLC field and MLC fields of $A_{\mathrm{MLC}} = 4 \times 4 - 20 \times 20\ \mathrm{cm}^2$ for each of the jaw fields of $A_{\mathrm{jaw}} = 10 \times 10, 15 \times 15$ and $20 \times 20\ \mathrm{cm}^2$; (b) in case of wedge type= $1 - 3$ (15°, 30° and 45° wedges), we used MLC fields of $A_{\mathrm{MLC}} = 4 \times 4 - 20 \times 20\ \mathrm{cm}^2$ for each of the jaw fields of $A_{\mathrm{jaw}} = 10 \times 10, 15 \times 15$ and $20 \times 20\ \mathrm{cm}^2$; and (c) in case of wedge type = 4 (60° wedge), we used MLC fields of $A_{\mathrm{MLC}} = 4 \times 4 - 15 \times 15\ \mathrm{cm}^2$ for each of the jaw fields of $A_{\mathrm{jaw}} = 10 \times 10$ and $15 \times 15\ \mathrm{cm}^2$.

(0) Zero stage (*K*=0)

At this stage, for all values of $A^{\mathrm{in\_jaw}}_{\mathrm{MLC}}/A_{\mathrm{jaw}}$ and for all numbers of wedge type $= 0 - 4$, we set

$$W_{K=0}\left(A^{\mathrm{in\_jaw}}_{\mathrm{MLC}}/A_{\mathrm{jaw}}\,;\,\mathrm{wedge\ type}\right) = 0.055, \tag{D1}$$

where the numerical value of 0.055 is taken as appropriate. Then we construct the $\mathrm{CF}^{\mathrm{a}}_{K=0}$ factor (as the zero stage of $\mathrm{CF}^{\mathrm{a}}_{\mathrm{OPF}}$) as

$$\mathrm{CF}^{\mathrm{a}}_{K=0}\left(A^{\mathrm{in\_jaw}}_{\mathrm{MLC}}/A_{\mathrm{jaw}};\,\mathrm{wedge\ type}\right) = \exp\left[-\,W_{K=0}\left(A^{\mathrm{in\_jaw}}_{\mathrm{MLC}}/A_{\mathrm{jaw}}\,;\,\mathrm{wedge\ type}\right)\cdot\left\{1 - \left(A^{\mathrm{in\_jaw}}_{\mathrm{MLC}}/A_{\mathrm{jaw}}\right)\right\}\right]. \tag{D2}$$

However, we found that this $\mathrm{CF}^{\mathrm{a}}_{K=0}$ factor cannot always give accurate calculation results for all wedge types. Therefore, we let the series of W_K $(K = 1, 2, \cdots)$ continuing from the $W_{K=0}$ term be constructed as a function of $A^{\mathrm{in\_jaw}}_{\mathrm{MLC}}/A_{\mathrm{jaw}}$ for a given irradiation mode of wedge type. The

following is described by taking an irradiation mode of wedge type=2 (30° wedge), for example, for constructing expressions for $\mathrm{dev}^{\%}_{K=1,2,3}$ (Equations D4, D8 and D12).

(1) First stage (*K*=1)

Based on calculated PDD datasets yielded by the above $\mathrm{CF}^{\mathrm{a}}_{K=0}$ function, we produce the following expression for $f^{\%}_{K=1}$ that is related to the % deviations ($\mathrm{dev}^{\%}_{K=1}$) as

$$f^{\%}_{K=1}\left(A^{\mathrm{in\_jaw}}_{\mathrm{MLC}}/A_{\mathrm{jaw}};\text{wedge type}\right)=1-\mathrm{dev}^{\%}_{K=1}\left(A^{\mathrm{in\_jaw}}_{\mathrm{MLC}}/A_{\mathrm{jaw}};\text{wedge type}\right)/100, \quad \text{(D3)}$$

with

$$\mathrm{dev}^{\%}_{K=1}\left(A^{\mathrm{in\_jaw}}_{\mathrm{MLC}}/A_{\mathrm{jaw}};\text{wedge type}\right)=3.5196\left(A^{\mathrm{in\_jaw}}_{\mathrm{MLC}}/A_{\mathrm{jaw}}\right)^{2}-0.6425\left(A^{\mathrm{in\_jaw}}_{\mathrm{MLC}}/A_{\mathrm{jaw}}\right)-2.1610. \quad \text{(D4)}$$

with $R^2=0.918$ (coefficient of determination), where the function of $\mathrm{dev}^{\%}_{K=1}$ is yielded (Figure D1a) by analyzing the % deviation datasets using the least-squares method. Then the function of $W_{K=1}$ is constructed as

$$W_{K=1}\left(A^{\mathrm{in\_jaw}}_{\mathrm{MLC}}/A_{\mathrm{jaw}};\text{wedge type}\right)=$$
$$-\log\left[f^{\%}_{K=1}\left(A^{\mathrm{in\_jaw}}_{\mathrm{MLC}}/A_{\mathrm{jaw}};\text{wedge type}\right)\cdot\mathrm{CF}^{\mathrm{a}}_{K=0}\left(A^{\mathrm{in\_jaw}}_{\mathrm{MLC}}/A_{\mathrm{jaw}};\text{wedge type}\right)\right]/\left\{1-\left(A^{\mathrm{in\_jaw}}_{\mathrm{MLC}}/A_{\mathrm{jaw}}\right)\right\} \quad \text{(D5)}$$

Accordingly, the $\mathrm{CF}^{\mathrm{a}}_{K=1}$ factor can be derived as

$$\mathrm{CF}^{\mathrm{a}}_{K=1}\left(A^{\mathrm{in\_jaw}}_{\mathrm{MLC}}/A_{\mathrm{jaw}};\text{wedge type}\right)=\exp\left[-W_{K=1}\left(A^{\mathrm{in\_jaw}}_{\mathrm{MLC}}/A_{\mathrm{jaw}};\text{wedge type}\right)\cdot\left\{1-\left(A^{\mathrm{in\_jaw}}_{\mathrm{MLC}}/A_{\mathrm{jaw}}\right)\right\}\right]$$
$$=f^{\%}_{K=1}\left(A^{\mathrm{in\_jaw}}_{\mathrm{MLC}}/A_{\mathrm{jaw}};\text{wedge type}\right)\cdot\mathrm{CF}^{\mathrm{a}}_{K=0}\left(A^{\mathrm{in\_jaw}}_{\mathrm{MLC}}/A_{\mathrm{jaw}};\text{wedge type}\right). \quad \text{(D6)}$$

(2) Second stage (*K*=2)

Similarly, based on calculated PDD datasets yielded by the above $\mathrm{CF}^{\mathrm{a}}_{K=1}$ function, we produce the expression for $f^{\%}_{K=2}$ that is related to the $\mathrm{dev}^{\%}_{K=2}$ deviations (Figure D1b) as

$$f^{\%}_{K=2}\left(A^{\mathrm{in\_jaw}}_{\mathrm{MLC}}/A_{\mathrm{jaw}};\text{wedge type}\right)=1-\mathrm{dev}^{\%}_{K=2}\left(A^{\mathrm{in\_jaw}}_{\mathrm{MLC}}/A_{\mathrm{jaw}};\text{wedge type}\right)/100, \quad \text{(D7)}$$

with

$$\mathrm{dev}^{\%}_{K=2}\left(A^{\mathrm{in\_jaw}}_{\mathrm{MLC}}/A_{\mathrm{jaw}};\text{wedge type}\right)=-0.0160\left(A^{\mathrm{in\_jaw}}_{\mathrm{MLC}}/A_{\mathrm{jaw}}\right)^{2}+0.0918\left(A^{\mathrm{in\_jaw}}_{\mathrm{MLC}}/A_{\mathrm{jaw}}\right)-0.0719, \quad \text{(D8)}$$

with $R^2=0.0052$. Accordingly, we obtain

$$W_{K=2}\left(A^{\mathrm{in\_jaw}}_{\mathrm{MLC}}/A_{\mathrm{jaw}};\text{wedge type}\right)=$$
$$-\log\left[f^{\%}_{K=2}\left(A^{\mathrm{in\_jaw}}_{\mathrm{MLC}}/A_{\mathrm{jaw}};\text{wedge type}\right)\cdot\mathrm{CF}^{\mathrm{a}}_{K=1}\left(A^{\mathrm{in\_jaw}}_{\mathrm{MLC}}/A_{\mathrm{jaw}};\text{wedge type}\right)\right]/\left\{1-\left(A^{\mathrm{in\_jaw}}_{\mathrm{MLC}}/A_{\mathrm{jaw}}\right)\right\}. \quad \text{(D9)}$$

Consequently, the $\mathrm{CF}^{\mathrm{a}}_{K=2}$ factor can be derived as

$$\mathrm{CF}^{\mathrm{a}}_{K=2}\left(A^{\mathrm{in\_jaw}}_{\mathrm{MLC}}/A_{\mathrm{jaw}};\text{wedge type}\right)=\exp\left[-W_{K=2}\left(A^{\mathrm{in\_jaw}}_{\mathrm{MLC}}/A_{\mathrm{jaw}};\text{wedge type}\right)\cdot\left\{1-\left(A^{\mathrm{in\_jaw}}_{\mathrm{MLC}}/A_{\mathrm{jaw}}\right)\right\}\right]$$
$$=f^{\%}_{K=2}\left(A^{\mathrm{in\_jaw}}_{\mathrm{MLC}}/A_{\mathrm{jaw}};\text{wedge type}\right)\cdot f^{\%}_{K=1}\left(A^{\mathrm{in\_jaw}}_{\mathrm{MLC}}/A_{\mathrm{jaw}};\text{wedge type}\right)\cdot\mathrm{CF}^{\mathrm{a}}_{K=0}\left(A^{\mathrm{in\_jaw}}_{\mathrm{MLC}}/A_{\mathrm{jaw}};\text{wedge type}\right). \quad \text{(D10)}$$

(3) Third stage (*K*=3)

Similarly, based on calculated PDD datasets yielded by the above $\mathrm{CF}^{\mathrm{a}}_{K=2}$ function, we produce the expression for $f^{\%}_{K=3}$ that is related to the $\mathrm{dev}^{\%}_{K=3}$ deviations (Figure D1c) as

$$f^{\%}_{K=3}\left(A^{\mathrm{in\_jaw}}_{\mathrm{MLC}}/A_{\mathrm{jaw}};\text{wedge type}\right)=1-\mathrm{dev}^{\%}_{K=3}\left(A^{\mathrm{in\_jaw}}_{\mathrm{MLC}}/A_{\mathrm{jaw}};\text{wedge type}\right)/100, \tag{D11}$$

with

$$\mathrm{dev}^{\%}_{K=3}\left(A^{\mathrm{in\_jaw}}_{\mathrm{MLC}}/A_{\mathrm{jaw}};\text{wedge type}\right)$$
$$=-0.0004\left(A^{\mathrm{in\_jaw}}_{\mathrm{MLC}}/A_{\mathrm{jaw}}\right)^{2}+0.001\left(A^{\mathrm{in\_jaw}}_{\mathrm{MLC}}/A_{\mathrm{jaw}}\right)-0.0007, \tag{D12}$$

with $R^2=3\mathrm{E}-07$. We have $f^{\%}_{K=3}\cong 1$ for all values of $A^{\mathrm{in\_jaw}}_{\mathrm{MLC}}/A_{\mathrm{jaw}}$. This means that the deviations of $\mathrm{dev}^{\%}_{K=3}$ are almost all composed of random errors. Accordingly, we may be able to state that the following $\mathrm{CF}^{\mathrm{a}}_{K=3}$ factor can produce reasonable calculation results. This factor can be derived as

$$\mathrm{CF}^{\mathrm{a}}_{K=3}\left(A^{\mathrm{in\_jaw}}_{\mathrm{MLC}}/A_{\mathrm{jaw}};\text{wedge type}\right)=\exp\left[-W_{K=3}\left(A^{\mathrm{in\_jaw}}_{\mathrm{MLC}}/A_{\mathrm{jaw}};\text{wedge type}\right)\cdot\left\{1-\left(A^{\mathrm{in\_jaw}}_{\mathrm{MLC}}/A_{\mathrm{jaw}}\right)\right\}\right]=$$
$$f^{\%}_{K=3}\left(A^{\mathrm{in\_jaw}}_{\mathrm{MLC}}/A_{\mathrm{jaw}};\text{wedge type}\right)\cdot f^{\%}_{K=2}\left(A^{\mathrm{in_{jaw}}}_{\mathrm{MLC}}/A_{\mathrm{jaw}};\text{wedge type}\right)\cdot f^{\%}_{K=1}\left(A^{\mathrm{in_{jaw}}}_{\mathrm{MLC}}/A_{\mathrm{jaw}};\text{wedge type}\right)\cdot$$
$$\mathrm{CF}^{\mathrm{a}}_{K=0}\left(A^{\mathrm{in_{jaw}}}_{\mathrm{MLC}}/A_{\mathrm{jaw}};\text{wedge type}\right). \tag{D13}$$

The present study utilized the $\mathrm{CF}^{\mathrm{a}}_{K=3}$ function at this stage (*K*=3) as the $\mathrm{CF}^{\mathrm{a}}_{\mathrm{OPF}}$ function in Equations 43 and 46, also for the other wedge types than wedge type=2 (30° wedge).

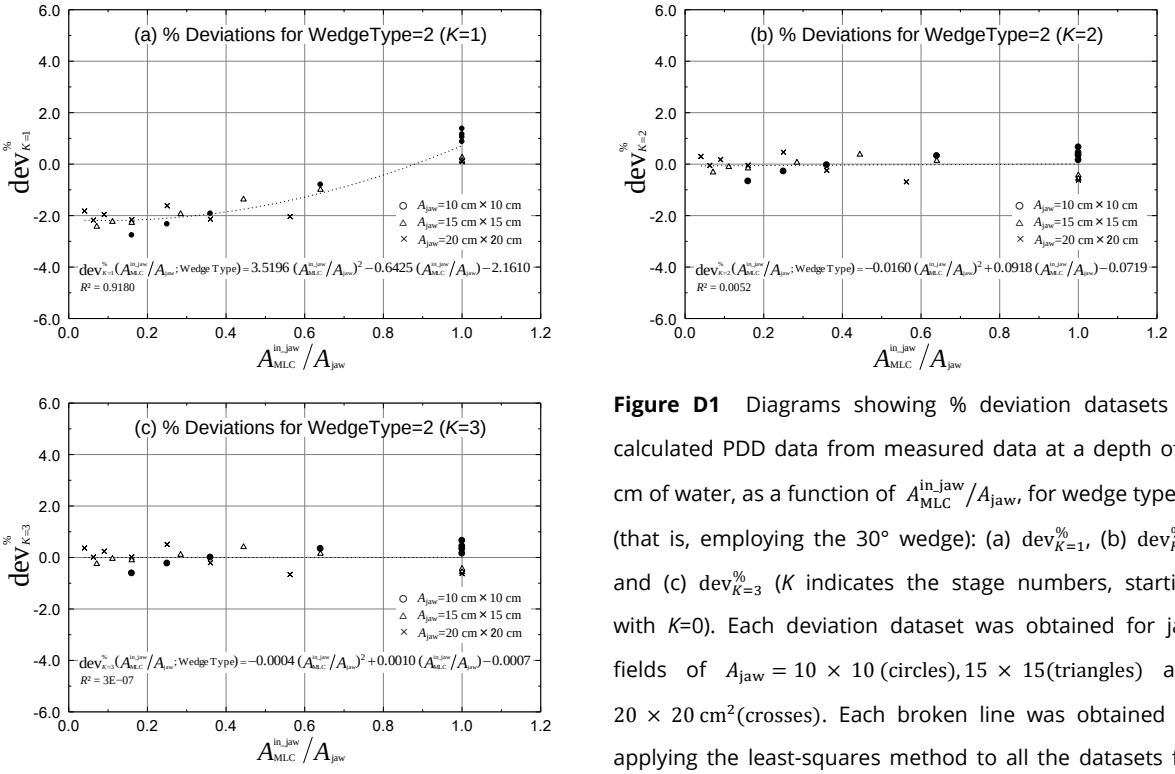

Figure D1 Diagrams showing % deviation datasets of calculated PDD data from measured data at a depth of 3 cm of water, as a function of $A^{\mathrm{in\_jaw}}_{\mathrm{MLC}}/A_{\mathrm{jaw}}$, for wedge type=2 (that is, employing the 30° wedge): (a) $\mathrm{dev}^{\%}_{K=1}$, (b) $\mathrm{dev}^{\%}_{K=2}$ and (c) $\mathrm{dev}^{\%}_{K=3}$ (*K* indicates the stage numbers, starting with *K*=0). Each deviation dataset was obtained for jaw fields of $A_{\mathrm{jaw}}=10\times 10\,(\mathrm{circles}),15\times 15(\mathrm{triangles})$ and $20\times 20\,\mathrm{cm}^2(\mathrm{crosses})$. Each broken line was obtained by applying the least-squares method to all the datasets for the three jaw fields.

Lastly, we summarize expressions for $\mathrm{dev}^{\%}_{K=1}$, $\mathrm{dev}^{\%}_{K=2}$ and $\mathrm{dev}^{\%}_{K=3}$ for wedge type=0–4, as follows:

(0) For no wedge (wedge type=0)

$$\mathrm{dev}^{\%}_{K=1} = 2.5583\left(A^{\mathrm{in\_jaw}}_{\mathrm{MLC}}/A_{\mathrm{jaw}}\right)^2 + 1.9668\left(A^{\mathrm{in\_jaw}}_{\mathrm{MLC}}/A_{\mathrm{jaw}}\right) - 4.8215 \quad (R^2 = 0.961),$$

$$\mathrm{dev}^{\%}_{K=2} = -0.2036\left(A^{\mathrm{in\_jaw}}_{\mathrm{MLC}}/A_{\mathrm{jaw}}\right)^2 + 0.3785\left(A^{\mathrm{in\_jaw}}_{\mathrm{MLC}}/A_{\mathrm{jaw}}\right) - 0.2507 \quad (R^2 = 0.0245),$$

$$\mathrm{dev}^{\%}_{K=3} = -0.0739\left(A^{\mathrm{in\_jaw}}_{\mathrm{MLC}}/A_{\mathrm{jaw}}\right)^2 + 0.0549\left(A^{\mathrm{in\_jaw}}_{\mathrm{MLC}}/A_{\mathrm{jaw}}\right) - 0.0081 \quad (R^2 = 0.0011).$$

(1) For the 15° wedge (wedge type=1)

$$\mathrm{dev}^{\%}_{K=1} = 2.8392\left(A^{\mathrm{in\_jaw}}_{\mathrm{MLC}}/A_{\mathrm{jaw}}\right)^2 + 1.0305\left(A^{\mathrm{in\_jaw}}_{\mathrm{MLC}}/A_{\mathrm{jaw}}\right) - 3.6205 \quad (R^2 = 0.9777),$$

$$\mathrm{dev}^{\%}_{K=2} = -0.1063\left(A^{\mathrm{in\_jaw}}_{\mathrm{MLC}}/A_{\mathrm{jaw}}\right)^2 + 0.2446\left(A^{\mathrm{in\_jaw}}_{\mathrm{MLC}}/A_{\mathrm{jaw}}\right) - 0.1317 \quad (R^2 = 0.0343),$$

$$\mathrm{dev}^{\%}_{K=3} = 0.0004\left(A^{\mathrm{in\_jaw}}_{\mathrm{MLC}}/A_{\mathrm{jaw}}\right)^2 - 0.0016\left(A^{\mathrm{in\_jaw}}_{\mathrm{MLC}}/A_{\mathrm{jaw}}\right) + 0.0011 \quad (R^2 = 3\mathrm{E}{-}06).$$

(2) For the 30° wedge (wedge type=2)

$$\mathrm{dev}^{\%}_{K=1} = 3.5196\left(A^{\mathrm{in\_jaw}}_{\mathrm{MLC}}/A_{\mathrm{jaw}}\right)^2 - 0.6425\left(A^{\mathrm{in\_jaw}}_{\mathrm{MLC}}/A_{\mathrm{jaw}}\right) - 2.1610 \quad (R^2 = 0.918),$$

$$\mathrm{dev}^{\%}_{K=2} = -0.0160\left(A^{\mathrm{in\_jaw}}_{\mathrm{MLC}}/A_{\mathrm{jaw}}\right)^2 + 0.0918\left(A^{\mathrm{in\_jaw}}_{\mathrm{MLC}}/A_{\mathrm{jaw}}\right) - 0.0719 \quad (R^2 = 0.0052),$$

$$\mathrm{dev}^{\%}_{K=3} = -0.0004\left(A^{\mathrm{in\_jaw}}_{\mathrm{MLC}}/A_{\mathrm{jaw}}\right)^2 + 0.001\left(A^{\mathrm{in\_jaw}}_{\mathrm{MLC}}/A_{\mathrm{jaw}}\right) - 0.0007 \quad (R^2 = 3\mathrm{E}{-}07).$$

(3) For the 45° wedge (wedge type=3)

$$\mathrm{dev}^{\%}_{K=1} = 3.6778\left(A^{\mathrm{in\_jaw}}_{\mathrm{MLC}}/A_{\mathrm{jaw}}\right)^2 - 0.7701\left(A^{\mathrm{in\_jaw}}_{\mathrm{MLC}}/A_{\mathrm{jaw}}\right) - 3.7162 \quad (R^2 = 0.8993),$$

$$\mathrm{dev}^{\%}_{K=2} = 0.115\left(A^{\mathrm{in\_jaw}}_{\mathrm{MLC}}/A_{\mathrm{jaw}}\right)^2 + 0.0014\left(A^{\mathrm{in\_jaw}}_{\mathrm{MLC}}/A_{\mathrm{jaw}}\right) - 0.1188 \quad (R^2 = 0.0123),$$

$$\mathrm{dev}^{\%}_{K=3} = 0.0085\left(A^{\mathrm{in\_jaw}}_{\mathrm{MLC}}/A_{\mathrm{jaw}}\right)^2 - 0.0103\left(A^{\mathrm{in\_jaw}}_{\mathrm{MLC}}/A_{\mathrm{jaw}}\right) + 0.0022 \quad (R^2 = 3\mathrm{E}{-}06).$$

(4) For the 60° wedge (wedge type=4)

$$\mathrm{dev}^{\%}_{K=1} = 2.6296\left(A^{\mathrm{in\_jaw}}_{\mathrm{MLC}}/A_{\mathrm{jaw}}\right)^2 + 0.8682\left(A^{\mathrm{in\_jaw}}_{\mathrm{MLC}}/A_{\mathrm{jaw}}\right) - 2.0372 \quad (R^2 = 0.9459),$$

$$\mathrm{dev}^{\%}_{K=2} = -0.0882\left(A^{\mathrm{in\_jaw}}_{\mathrm{MLC}}/A_{\mathrm{jaw}}\right)^2 + 0.1456\left(A^{\mathrm{in\_jaw}}_{\mathrm{MLC}}/A_{\mathrm{jaw}}\right) - 0.0628 \quad (R^2 = 0.0027),$$

$$\mathrm{dev}^{\%}_{K=3} = -0.0002\left(A^{\mathrm{in\_jaw}}_{\mathrm{MLC}}/A_{\mathrm{jaw}}\right)^2 + 0.001\left(A^{\mathrm{in\_jaw}}_{\mathrm{MLC}}/A_{\mathrm{jaw}}\right) - 0.0007 \quad (R^2 = 6\mathrm{E}{-}07).$$